JOURNAL OF CLINICAL MICROBIOLOGY, Dec. 2006, p. 4345–4352 Vol. 44, No. 12
0095-1137/06/$08.00+0 doi:10.1128/JCM.00577-06

Neurologic Disease in Captive Lions (*Panthera leo*) with Low-Titer Lion Lentivirus Infection▽

Greg Brennan,[1]† Michael D. Podell,[2] Raymund Wack,[3]‡ Susan Kraft,[4] Jennifer L. Troyer,[1]§ Helle Bielefeldt-Ohmann,[1] and Sue VandeWoude[1]*

Departments of Microbiology, Immunology, and Pathology[1] and Environmental and Radiologic Health Sciences,[4] Colorado State University, Fort Collins Colorado 80523; Department of Veterinary Clinical Sciences, The Ohio State University, Columbus, Ohio 43210[2]; and Department of Medicine and Epidemiology, University of California, Davis, California 95616-8747[3]

Received 17 March 2006/Returned for modification 23 July 2006/Accepted 17 September 2006

Lion lentivirus (LLV; also known as feline immunodeficiency virus of lion, *Panthera leo* [FIVPle]) is present in free-ranging and captive lion populations at a seroprevalence of up to 100%; however, clinical signs are rarely reported. LLV displays up to 25% interclade sequence diversity, suggesting that it has been in the lion population for some time and may be significantly host adapted. Three captive lions diagnosed with LLV infection displayed lymphocyte subset alterations and progressive behavioral, locomotor, and neuroanatomic abnormalities. No evidence of infection with other potential neuropathogens was found. Antemortem electrodiagnostics and radiologic imaging indicated a diagnosis consistent with lentiviral neuropathy. PCR was used to determine a partial lentiviral genomic sequence and to quantify the proviral burden in eight postmortem tissue specimens. Phylogenetic analysis demonstrated that the virus was consistent with the LLV detected in other captive and free-ranging lions. Despite progressive neurologic signs, the proviral load in tissues, including several regions of the brain, was low; furthermore, gross and histopathologic changes in the brain were minimal. These findings suggest that the symptoms in these animals resulted from nonspecific encephalopathy, similar to human immunodeficiency virus, FIV, and simian immunodeficiency virus (SIV) neuropathies, rather than a direct effect of active viral replication. The association of neuropathy and lymphocyte subset alterations with chronic LLV infection suggests that long-term LLV infection can have detrimental effects for the host, including death. This is similar to reports of aged sootey mangabeys dying from diseases typically associated with end-stage SIV infection and indicates areas for further research of lentiviral infections of seemingly adapted natural hosts, including mechanisms of host control and viral adaptation.

Lion lentivirus (LLV; also known as feline immunodeficiency virus [FIV] of lion, *Panthera leo* [FIVPle]) is an FIV that is related to yet distinct from the domestic cat (*Felis catus*) FIV (4, 52). LLV is present in free-ranging prides at seroprevalence rates that approach 100% and is commonly detected in captive lion (*Panthera leo*) populations, suggesting that it is efficiently transmitted (4, 19, 22, 25, 32, 42, 50, 52, 53). Five distinct heterogeneous clades of LLV have been identified on the basis of sequence analysis of a conserved region of the *pol* gene. Up to 25% sequence diversity between clades has been noted in this highly conserved region of the lentiviral genome, suggesting that, for such genetic heterogeneity to occur, this virus has infected the lion population for a considerable time (4, 52, 53). LLV apparently causes little or no clinical disease in free-ranging lions, although clinical signs and immunopathology reminiscent of lentiviral infection have been reported in geriatric captive animals, perhaps due to their longer life spans and/or stress-related cofactors in these cohorts (6, 19, 22, 41, 42).

The effects of FIV on domestic cats are well documented and most notably include infection of $CD4^+$ T cells with subsequent CD4-CD8 inversion and immunosuppression, making it a useful model for the pathogenesis of human immunodeficiency virus (HIV) infection (13, 17). FIV also induces a lentiviral encephalopathy and has been used in this capacity as a model for HIV neurologic disease (36–41).

Information on the tissue tropism, viral kinetics, and pathogenesis of LLV is much more limited in scope. Lymphoma in one lion and retinitis in several LLV-infected lions have been described, and T-cell-subset profile alterations have been substantiated in several captive lions (6, 19, 22, 42) and in free-ranging individuals (46). This study describes the neurologic manifestations of lion lentivirus infection in three captive lions, which were found to be analogous to FIV and HIV neuropathies, and characterizes the viral distribution and selected immunological phenotypes associated with LLV infection. These findings illustrate an association between chronic LLV infection and clinical neurologic disease in lions, despite a low viral load, analogous to the lentiviral encephalopathy in cats and humans, and also provides insights into the viral load and distribution that contribute to the relatively low level of pathogenicity of this virus for its natural host.

* Corresponding author. Mailing address: Department of Microbiology, Immunology, and Pathology, Colorado State University, 1619 Campus Delivery, Fort Collins, CO 80523-1619. Phone: (970) 491-7162. Fax: (970) 491-0523. E-mail: suev@lamar.colostate.edu.

† Present address: Department of Microbiology, University of Washington, Seattle, WA 98195.

‡ Present address: Sacramento Zoo, 3900 Land Park Dr., Sacramento, CA 95822.

§ Present address: Laboratory of Genomic Diversity, SAIC-Frederick, Inc., NCI-Frederick, Frederick, MD 21702.

▽ Published ahead of print on 27 September 2006.

MATERIALS AND METHODS

Animals. Two adult female LLV-seropositive lions (lions EL and DJ) and one adult male LLV-seropositive lion (lion TT) from the Columbus Zoo in Columbus, OH, were evaluated in this study. The approximate ages of lions EL, DJ, and TT at the initiation of these studies were 19, 17, and 15 years, respectively. Three seronegative lions, one female and two males, ages 18, 21, and 23 months, served as uninfected control blood donors. All animals were housed at the Columbus Zoo in two separate exhibits. The three infected lions were physically separated from the control lions by approximately 1/4 mile. No utensils or equipment were shared between the exhibits. All lions were fed a commercial carnivore diet (5 to 9 pounds; Zoo Carnivore Diet; Dallas Crown Inc., Kaufman, TX) daily, with a fast day on Sunday. Both infected female lions were euthanized because of progressive physical deterioration, while the male died due to a severe progressive anemia. The studies described here were approved by the Ohio State University, the Columbus Zoo, and the Colorado State University Animal Care and Use Committees.

Physical examination and observation. General health evaluation consisted of serum biochemical profile analysis, complete blood count with differential analysis, platelet count, urinalysis, hemostasis screening (one-stage prothrombin time, activated partial thromboplastin time, fibrinogen, fibrin degradation products), and thoracic radiographs performed at the Ohio State University Veterinary Teaching Hospital (Columbus, OH). Observational changes in the behaviors and activities of lions TT and EL were assessed on a monthly basis by Columbus Zoo animal handlers. Selected elapsed-time videos were reviewed by a veterinary neurologist (M.D.P.). The frequencies of behavior changes were scored on a discrete scale from 0 to 3, as follows: 0, normal behavior (normal mentation and appetite); 1, mild behavior change (very slight dysphagia and a slight change in normal behavior, such as a delay in shifting cages); 2, moderate behavior change (obvious dysphagia not impeding consumption of diet, behavior change in normal routine shifting or training, slight imbalances when jumping or climbing, and/or "star gazing" [explained below] that was easily interrupted); and 3, severe change (agitation in a normally calm animal, star gazing that was difficult to interrupt, excessive stereotypic behavior, dysphagia that significantly increased the time required to consume food, and/or obvious incoordination).

Electrodiagnostic examination. Quantitative neurophysiologic changes were analyzed by using auditory evoked potential (AEP) and quantitative electroencephalography (QEEG) tests performed while the animals were under isoflurane gas anesthesia by use of the Biologic Brain Atlas system (Biologic System Co., Mundelein, IL). Venous blood gas, pulse oximetry, and end-tidal partial CO_2 pressure were monitored to stabilize the blood pH and ensure constant levels of arterial oxygen and carbon dioxide tension to remove confounding variables of the QEEG. The QEEG data were analyzed by comparison of the spectral analysis results for the infected and the control animals within each group and between groups (36). Spectral differences between hemispheres for each individual recording were evaluated during each recording session. Electrode placement, signal filtering, and averaging and data analysis for AEP were performed as described previously (39) by using a computerized electrodiagnostic system (Neuropak 4; Nihon-Kodon, Irvine, CA).

Neuroimaging. Magnetic resonance imaging (MRI) of the brain was performed with one affected female lion (lion EL) by using a 0.3-T open-magnet MRI system (AIRIS; Hitachi Medical Systems America Inc., Twinsburg, OH). The lion was positioned in sternal recumbency while she was under general isoflurane anesthesia. The MRI study included transverse dual-spin echo proton density and spin-spin relaxation time (T2)-weighted images (repetition time = 3,170 ms, time to echo = 25 and 90 ms, slice thickness = 5 mm) and pre- and postcontrast sagittal, dorsal, and transverse spin-lattice relaxation time (T1)-weighted images (repetition time = 600 ms, time to echo = 25 ms, slice thickness = 5 mm). The contrast medium was intravenously administered gadopentetate-dimeglumine (0.2 mg/kg of body weight; Magnevist; Berlex Laboratories, Wayne, NJ).

Lymphocyte phenotyping. The immune profiles of all infected lions were monitored by lymphocyte subtype analysis and determination of total granulocyte counts at four time points during one 9-month period after clinical signs were recognized. Lymphocyte subpopulations were enumerated by immunostaining and flow cytometry with an Epics Elite flow cytometer (Beckman Coulter, Inc., Miami, FL; Department of Veterinary Biosciences, The Ohio State University, Columbus, OH). Mouse anti-cat CD8 and CD4 (Southern Biotech, Birmingham, AL) and CD5 (clone f43, Abcam, Cambridge, MA; (1) were used to stain fresh whole blood, as described previously (36). The lymphocyte totals, expressed as pan-T, $CD4^+$, and $CD8^+$ lymphocytes, were determined by multiplying the percentage of positively immunostaining populations by the complete blood count lymphocyte values.

Serology. The titers of antibodies to LLV in serum were determined by immunoblotting, as described previously (55). Feline leukemia virus titers were determined by enzyme-linked immunosorbent assay (Ohio State University Veterinary Teaching Hospital Clinical Laboratory). Assays for the detection of serum and cerebrospinal antibodies to canine distemper virus, feline infectious peritonitis virus, *Toxoplasma gondii*, *Neospora caninum*, and cryptococcosis were performed by the Laboratory Corporation of America (Dublin, OH).

Postmortem evaluation. The animals were subjected to a postmortem examination immediately following euthanasia, and gross lesions were noted at that time. At necropsy, samples were collected from the following tissues: brain, pituitary, meninges, trigeminal ganglia, spinal cord, radial nerve, eye, pancreas, liver, gall bladder, stomach, small and large intestines, lymph nodes, heart, lungs, kidney, thyroid, parathyroid, adrenal gland, skeletal muscle, tongue, tendon, bone marrow, and skin. Samples of each tissue were fixed in 10% neutral buffered formaldehyde for 4 days and were then embedded in paraffin. Sections of 5 to 6 μm from each tissue were stained with hematoxylin and eosin and examined on an Olympus BX41 microscope equipped with a Q-Color-3 camera and corresponding software (Olympus, Center Valley, PA).

Virology. (i) In vitro propagation. One million peripheral blood mononuclear cells (PBMCs) from lions TT and EL were collected at three time points and cocultivated with an equal number of the following cell types by standard techniques: domestic cat PBMCs, naïve lion PBMCs, naïve puma (*Puma concolor*) PBMCs, the 3201 interleukin-2-independent feline lymphoid cell line, the GS-355 feline astrocyte cell line, and Crandall feline kidney cells (CRFKs; CCL-94, American Type Culture Collection, Manassas, VA) (55). Supernatants were collected biweekly and were assayed for reverse transcriptase (RT) activity between days 14 and 35 of culture by using a microtiter RT assay (18, 58). FIV-infected CRFK supernatants and uninfected cell cultures served as positive and negative controls, respectively.

(ii) DNA sequencing. DNA was extracted from the lion TT PBMCs and subjected to degenerate PCR with consensus primers to amplify a 385-bp sequence in *pol* corresponding to the FIV Petaluma coordinates from base pairs 2529 to 2934 (4). The PCR products were cloned by using a Topo TA kit (Invitrogen, Carlsbad, CA) and were sequenced by Macromolecular Resources (Fort Collins, CO). Nested primers were generated from this lion TT *pol* sequence (outer forward primer, 5′-ACAGAAAAGGGTGCAGAAG; outer reverse primer, 5′-GGCAAAGAACACCATACAAA; inner forward primer, 5′-GGGTGCAGAAGTTCAAT; inner reverse primer, 5′-TTATTCACCTTCGGTAAAGT). The outer and the inner primers amplified fragments of 180 bp and 133 bp, respectively. These primers were used to generate PCR products from lion EL, which were similarly cloned and sequenced.

(iii) Phylogenetic analysis. A total of 350 bp of the amplified sequence was aligned to the LLV sequences of known subtype by use of the ClustalX program. Two domestic cat FIV sequences were included as the outgroup. Phylogenetic reconstruction was performed by using PAUP, version 4.0 (51). The minimum-evolution (ME) and the maximum-likelihood (ML) methods were used for tree reconstruction, with starting trees obtained by neighbor joining, followed by use of a tree-bisection reconnection branch swapping algorithm. The Tajima-Nei base substitution algorithm was used for ME analysis; estimated general time-reversible substitution frequencies, corrected for among-site rate variations (gamma distribution) and a proportion of invariant sites, were used for ML analysis. Both methods placed the new LLV sequence in the same clade and produced trees with similar topologies. A bootstrap analysis consisting of 1,000 repetitions was conducted for the distance-based analysis (ME analysis), as described previously (52).

(iv) Proviral load and tissue distribution. Multiple cell and tissue samples (PBMCs and liver, spleen, peripheral lymph node, cerebellum, frontal cortex, parietal lobe, and bone marrow tissues) were collected from lion TT at necropsy. Lions DJ and EL did not have planned necropsies, and therefore, the harvesting of tissue for DNA extraction was not conducted. DNA was extracted from each tissue by using a QIAamp DNA blood mini kit (QIAGEN, Valencia, CA). Serial 10-fold dilutions of DNA from each tissue were made from 1 μg to 1 pg. The nested primers generated from lion TT's *pol* sequence were used to amplify a 133-bp sequence in a three-round nested touchdown PCR assay (15, 45, 57) by using the conditions described below with a Perkin-Elmer Gene Amp PCR system 9600 thermocycler.

In round 1, the reaction mixture comprised DNA, 0.2 mM deoxynucleoside triphosphates, 3 mM $MgCl_2$, 4 μM each outer primer, and 2.5 mU of *Taq* polymerase (Sigma Co., St. Louis, MO) in a final volume of 25 μl with 1× reaction buffer (Sigma Co.). Cycling parameters consisted of 1 min at 94°C, 94°C for 10 s, and 72°C for 20 s and then 2 cycles of 60°C and 48°C for 20 s, followed by 15 cycles with 45°C extensions for 20 s. In rounds 2 and 3, the reaction mixture comprised 1 μl of the product from the previous round, 0.2 mM deoxynucleoside

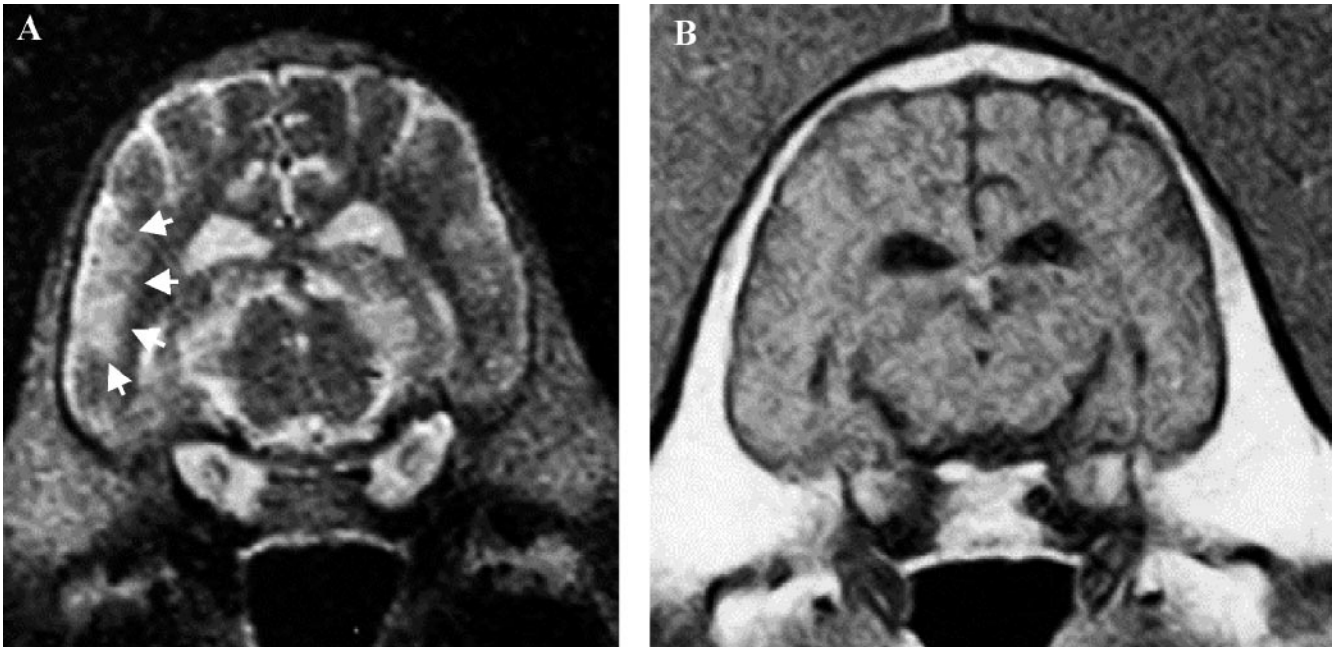

FIG. 1. Imaging reveals changes in the brains of LLV-infected lions. (A) Transverse T2-weighted magnetic resonance image at the level of the parietal lobes of the brain of lion EL. There are bilateral multiple patchy hyperintensities throughout the parietal and temporal cortex, and these are most extensive on the right (arrows). Sulci are prominent, and lateral ventricles are mildly enlarged. (B) Transverse T1-weighted magnetic resonance image from the identical level of the parietal lobes of lion EL's brain. The corresponding parietal and temporal cortexes are isointense to slightly hypointense and nonenhancing on T1-weighted images.

triphosphates, 3.5 mM $MgCl_2$, 4 μM each primer, and 2.5 mU of *Taq* polymerase (Sigma Co.) in a final volume of 30 μl with 1× reaction buffer (Sigma Co.). Cycling parameters consisted of 1 min 94°C, 94°C for 10 s, and 72°C for 20 s and then 2 cycles of 60°C and 48°C for 20 s, followed by 10 cycles with 45°C extensions for 20 s. Titration endpoints were determined for each tissue by evaluating the lowest dilution that reproducibly amplified a PCR product. The lowest 10-fold dilution that resulted in an amplified product was then diluted twofold in a serial manner to more closely determine the dilutional endpoint. Each trial was repeated at least twice in duplicate or triplicate, and the same endpoint was obtained during each trial. Proviral copy numbers per 10^6 cells were calculated by assuming that 1 μg of DNA was representative of 10^5 cells. This assay was determined to be sensitive to between 10 and 100 proviral copies/μg DNA by titration of target plasmid dilutions spiked in 1 μg of naïve DNA (data not shown).

RESULTS

Physical examination and observation. All three LLV-infected lions developed progressive weight loss and mild lymphadenopathy over the 3-year course of observation. All infected lions were found to display periodic "star-gazing" behavior of various durations. This behavior consisted of motionless staring into the sky with a lack of response to stimuli. Other behavioral changes found in the LLV-infected lions included dysphagia, abnormal gait, and ataxia. Periods of lethargy were also noted. Both lion TT and lion EL displayed a progressive increase in observed abnormal behavioral scoring during the course of this study.

Electrodiagnostic examination. LLV-infected lions demonstrated abnormalities by AEP and QEEG testing. Prolonged peak-onset latencies of waves III and V and interpeak latencies compared to the 95% confidence intervals of the values for the control lions were seen for the AEPs of all LLV-infected lions, indicating altered brain stem pathway function. The infected lions also demonstrated an increase in diffuse slow-wave activity compared to that for the control animals (data not shown).

Neuroimaging. Abnormal MRI findings included patchy cortical and subcortical white matter asymmetrical hyperintensities of the parietal and temporal lobes on T2-weighted images (Fig. 1A). Those areas were isointense on the T1-weighted images and were nonenhancing (Fig. 1B). No mass effect was present. Sulci were prominent, and there was mild ex vacuo ventriculomegaly, consistent with cerebrocortical atrophy (Fig. 1B). These MRI findings were consistent with chronic encephalopathy from encephalomalacia or encephalitis.

Serology and immunophenotyping. All lions were seronegative for feline leukemia virus, canine distemper virus, feline infectious peritonitis virus, *Toxoplasma gondii*, *Neospora caninum*, and cryptococcosis. The titers of antibodies against LLV antigens in serum were 1:800 for lion EL and >1:1,600 for lion TT; control lion sera were negative at 1:50. Lion DJ was not tested for antibodies to LLV but was positive by an FIV-specific enzyme-linked immunosorbent assay. All LLV-infected lions demonstrated persistent lymphopenia and abnormalities in CD4 and CD8 T-cell counts (Table 1). For lion DJ, only one sample was evaluated for the T-cell phenotype, and it was taken just prior to necropsy. This sample had marked decreases in $CD4^+$ and $CD8^+$ T-cell counts relative to those for the LLV-negative controls. Four sequential samples from lion EL demonstrated normal $CD4^+$ T-cell counts but elevated $CD8^+$ T-cells counts. Two samples from lion TT had low $CD4^+$ T-cell counts and normal to high $CD8^+$ T-cell counts. CD4:CD8 ratios averaged less than 2 for all three LLV-posi-

TABLE 1. $CD4^+$ lymphocyte counts and the CD4:CD8 ratio are altered in LLV-seropositive lions (DJ, EL, TT) compared with those in LLV-seronegative lions

Lion[a]	Range (mean)		
	$CD4^+$ lymphocyte count	$CD8^+$ lymphocyte count	CD4:CD8 ratio
DJ ($n = 1$)	162	131	1.2
EL ($n = 4$)	983 (270–1,284)	525 (427–624)	1.9 (0.5–2.1)
TT ($n = 2$)	105 (41–170)	470 (115–826)	0.3 (0.2–0.4)
Control ($n = 3$)	905 (693–1,198)	223 (182–278)	4.0 (3.8–4.2)

[a] n, number of samples tested.

tive animals, while the mean CD4:CD8 ratio for the LLV-negative animals was 4.

Postmortem evaluation. (i) Gross pathology. Lion TT presented in poor body condition, with marked icteric discoloration of the mucous membranes, fat, and viscera. Lion TT had pronounced splenomegaly and hepatomegaly; and the lion's lungs appeared to be congested, while the gastrointestinal tract appeared to be normal. The brain diplayed meningeal fibrosis, mild cortical atrophy of the frontal cortex, and mild bilateral ventriculomegaly of the third ventricles. In contrast, there were no grossly appreciable changes in the brains of lions EL and DJ and only minor aging-associated or chronic lesions in other organs, including biliary cysts in the liver, cataracts, alopecia, multifocal scarring in the lungs, and a thyroid adenoma in lion EL.

(ii) Micropathology. Neuropathologic abnormalities were found in all three LLV-seropositive animals but were generally mild. Severe focal fibrosis of the white matter, presumably of vascular adventitial origin in the corpus callosum and the adjacent cingulate gyrus, was noted in lion DJ. Lion TT had mild lymphocytic meningitis with vascular dilation and accumulation of monocytes-macrophages in the vascular lumina. Lion TT had widespread, but mild, neuronal degeneration and necrosis in the neocortex, accompanied by minimal to mild microgliosis. In a focally extensive area of the subventricular neuropil in the left thalamus there was malacia with cavitation, hemorrhage, and infiltration of macrophages (Fig. 2). Throughout many parts of the brain, but most notably in the thalamus, there was also perivascular accumulation of hemosiderin-containing macrophages, suggestive of an earlier hemorrhagic event(s). The histological changes seen in the central nervous system of lion EL were subtle and comprised vascular mineralization in the meninges and choroid plexus and minimal to mild myelodegenerative changes in the spinal cord, including scattered axonal sheath or axonal swelling and rare axonophagia.

Virology. LLV was not recovered from any in vitro cocultures. However, a 385-bp LLV *pol* sequence was amplified from lion TT, and nested primers designed from this fragment isolated a 133-bp *pol* sequence from lion EL that was identical to that from lion TT except at 1 bp. The sequence of a 350-bp fragment from lion TT was compared to previously published lion lentivirus sequences of known origin and subtype (52, 53) and was shown to fall clearly in the FIVPle subtype A clade (GenBank accession no. AY594655) (Fig. 3). This clade is widely distributed among free-ranging African lions (52, 53) and, interestingly, has also been found in captive lions and a captive snow leopard in Asian zoos (53).

The LLV proviral copy number, as quantified by the three-round touchdown PCR described in Materials and Methods, was extremely low in all tissues examined. The liver had the highest proviral load (837 copies/10^6 cells). Despite marked neurologic signs, the brain had very low to undetectable pro-

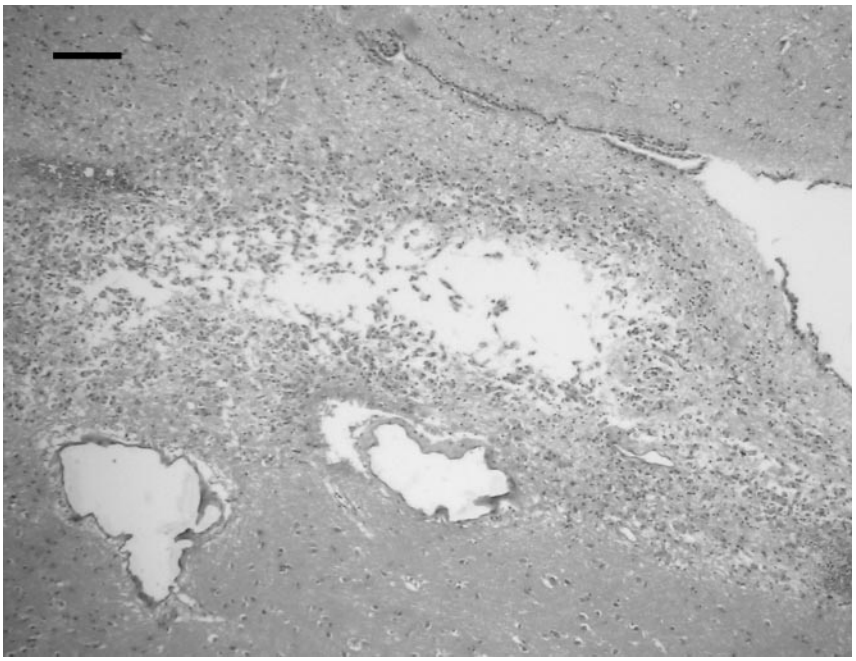

FIG. 2. Microscopic neuropathology of an LLV-infected lion. Neuropil malacia with cavitation, infiltration of macrophages, and multifocal hemorrhage in a subventricular area of the left thalamus of lion TT can be seen. Hematoxylin and eosin staining. Bar, 100 μm.

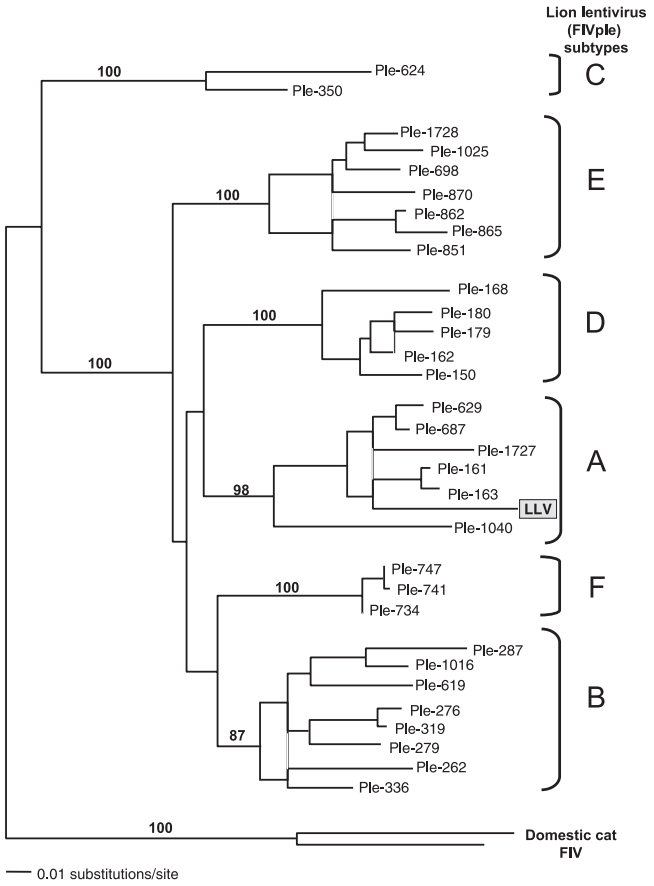

FIG. 3. Phylogenetic tree of LLV *pol* RT sequences (350 bp included in the analysis). A single minimum-evolution tree estimated by neighbor joining, with bootstrap support shown for relevant nodes, is illustrated. Boxed, shaded text designates the sequence isolated from our study lion; the Ple-*n* designations indicate sequences obtained from free-ranging and captive lions. Subtypes A to F, as defined by Troyer et al. (52), are indicated on the right. FIV Fca and FIV Petaluma are two domestic cat FIV strains used as an outgroup.

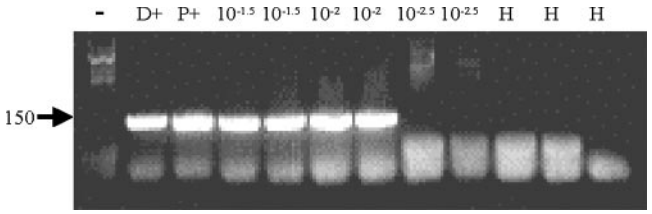

FIG. 4. Proviral DNA demonstrated by semiquantitative PCR. Liver from lion TT was collected at necropsy, DNA was extracted, and a three-round semiquantitative touchdown PCR was performed to quantify the tissue viral load, as described in the text. The product was run on an agarose gel, stained with ethidium bromide for visualization, and photographed. PCR products were detected at a $10^{-2.0}$ dilution of tissue but not at a $10^{-2.5}$ dilution of tissue. The results for all tissues are shown. Lane −, naïve domestic cat PBMC DNA; lane D+, LLV-infected domestic cat PBMC DNA; lane P+, plasmid containing a fragment of LLV *pol*; lanes H, water-only controls; lanes with numbers, dilution series of DNA used in the reaction.

viral levels in samples subjected to multiple amplification attempts (Fig. 4 and 5).

DISCUSSION

The three lions evaluated in this study displayed neurologic signs of disease both antemortem and postmortem, consistent with lentiviral neuropathies in other species, including humans and cats infected with HIV and FIV, respectively (12, 38). Magnetic resonance images of patients with HIV and FIV encephalopathy demonstrate cerebral atrophy and white matter lesions similar to those lesions found in lion EL (8, 10, 39, 43, 47). Similarly, the alterations in the AEP and the QEEG activities observed in these animals have been noted in humans with HIV infections and cats with FIV infections (31, 38, 39). The signs of vascular damage seen in the brains of two lions are consistent with those seem in the brains of HIV-infected patients (44) and simian immunodeficiency virus (SIV)-infected nonhuman primates (H. Bielefeldt-Ohmann et al., unpublished data), although the most typical histopathologic change seen in humans, multinucleated giant cells resulting from the fusion of activated macrophages and microglia, was not noted (12). However, the multiple functional and morphological similarities detected suggest that the neuropathologic mechanisms for the disease documented in these lions are consistent with lentiviral neuropathy. This is further supported by the fact that the results of serologic evaluations for a panel of pathogens associated with feline neurologic disease were negative, while LLV seropositivity, PCR positivity, and the immunopathology findings were consistent with active and clinical LLV disease.

Cats chronically infected with FIV (>3 years) typically have PBMC proviral burdens greater than 10^3 infected cells per million cells (13). In contrast, lion TT had only slightly more than 10^2 proviral copies per million PBMCs at death. Low proviral levels in the brain suggest an immune-mediated neuropathology rather than a direct effect of the virus. In humans, lentiviral encephalopathy has been shown to result primarily from metabolic and inflammatory damage rather than from viral replication. Microglia have been shown to be an important reservoir for HIV, and microglial satellitosis has been associated with axonal injury (10, 12, 21, 31). The principal mediator of these effects is the activated mononuclear phagocyte (MP; 10, 12, 21, 56). The neurotoxic effects are the result of the nonspecific inflammation induced by the release of proinflammatory cytokines, as well as the release of excitatory amino acids and other chemokines produced by MPs (16, 34). Additionally, infected astrocytes have decreased glutamate reuptake, while further release of glutamate is triggered by the activated MP (9, 23, 31). The HIV-1 Tat protein induces monocyte chemoattractant protein 1 expression in astrocytes, which results in further MP entry into the brain (9, 34, 59). Fas protein induction in host cells in response to HIV infection stimulates the further inflammation of astrocytes and acts as an apoptotic signal to neurons and microglia (23). Ultimately, these and other pathways result in widespread neuronal injury and death. Oxidative stress enhances the neurologic damage, resulting in a severe encephalopathy. Our findings suggest that even low levels of LLV replication may still ultimately result in overt fatal disease by a mechanism other than immunosuppression. This is reminiscent of what has been reported for patients receiving highly active antiretroviral therapy, who, despite hav-

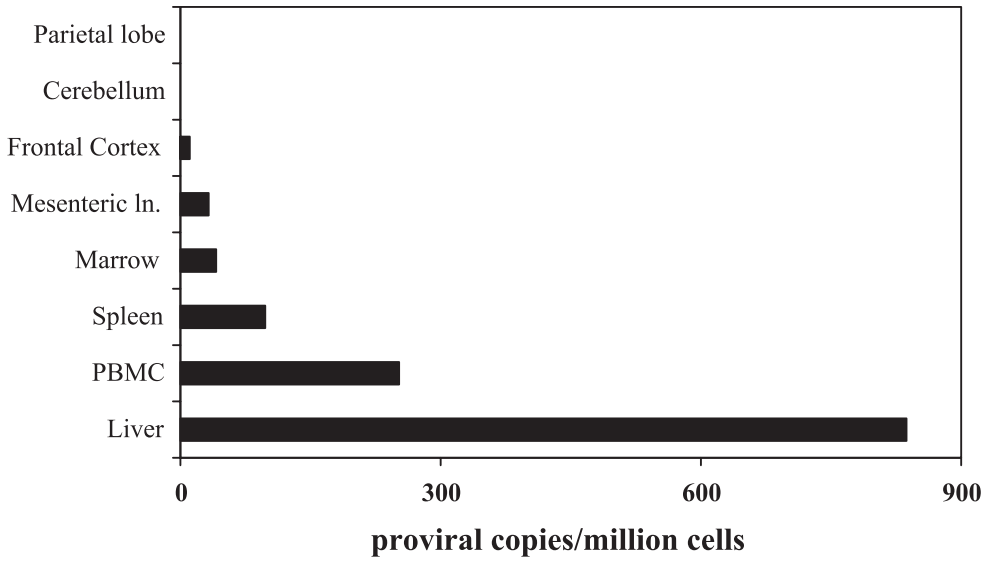

FIG. 5. LLV proviral load in tissues is low during end-stage disease. The LLV proviral DNA copy numbers from tissues collected from lion TT at necropsy are shown. The proviral DNA copy number per million cells was determined by titrating 1 μg of DNA, equivalent to 10^5 cells, by semiquantitative PCR with primers that amplified a conserved region of *pol*, as described in the text. All samples titrated to the same endpoint during multiple replicates; thus, standard deviation bars have not been included. ln., lymph node.

ing therapeutically controlled virus loads, develop central and peripheral neuropathies over time (26, 28, 30).

High titers of anti-LLV antibodies were detected in lions two lions for which antibodies were titrated, TT and EL. This is typical of the titers noted in other seropositive lions (S. VandeWoude, unpublished data). While the neutralizing abilities of these antibodies were not evaluated, the antibody response to this virus may have contributed to containment of the viral load, and it is possible that the robust antibody response contributed to immune-mediated damage in the brain. Anti-HIV type 1 (HIV-1) antibodies increase HIV-1 uptake into human monocytes and suggest that viral opsonization may be one mechanism for neuroinvasion in these animals (2); viral antigen-antibody complement-mediated vascular damage is a second mechanism recognized in HIV encephalopathy (44).

Consistent with the findings of other studies, we determined that antibodies recognizing domestic cat CD4, CD5, and CD8 surface antigens bound efficiently to lion PBMCs (5, 6, 22, 46). While the study described in this report did not use CD4 and CD8 dual staining, other studies have not identified $CD4^+$ $CD8^+$ double-positive cells in the circulation, as has been noted in some subspecies of African Green monkeys resistant to naturally occurring SIV disease (20, 29). The significant difference between the ages of the three infected animals and those of the three control lions may have contributed to the lymphocyte subset differences observed between the LLV-seropositive and the LLV-seronegative animals in this study. It has been difficult to overcome this analytical limitation in studies of LLV-associated immunopathology, as the majority of mature lions in captive and free-ranging settings are LLV positive. In two published reports that have enumerated CD4 and CD8 in lions, values were reported for five naïve lions aged 2, 3, 9, and unknown numbers of years (46) and five naïve lions aged 2 to 7 years (6). Both studies noted statistically significant decreases in $CD4^+$ T-cell counts in LLV-seropositive lions, as well as changes in $CD8^+$ T-cell distributions, concurrent with disease status, consistent with our findings.

The lymphocyte subset profiles observed in the animals in this study are consistent with immune dysregulation, analogous to that in HIV and FIV disease.

Interestingly, each lion demonstrated a different pattern of subsets, consistent with the different phases of AIDS that have been recognized in humans and cats. Lion DJ demonstrated severe lymphopenia and depletion of both $CD4^+$ and $CD8^+$ cells, consistent with end-stage AIDS. Lion EL had relatively normal $CD4^+$ T-cell counts but elevated $CD8^+$ T-cell counts, as might be noted in the steady-state phase of disease. Lion TT had an intermediate pattern of $CD4^+$ T-cell depletion and elevated $CD8^+$ T-cell counts, suggesting that T-cell disease expression in this animal was not controlled as well as it was in lion EL. As in HIV and FIV infections, it appears that the progression of disease in these lions is associated with changes in $CD4^+$ and $CD8^+$ T-cell dynamics, although the time to disease appears to be much longer in lions than in humans or domestic cats. Ultimately, at least in this cohort, neurologic disease and not immunodeficiency was the cause of death or the reason for euthanasia (4, 11, 13, 17, 42, 48).

Multiple attempts to propagate LLV in vitro were unsuccessful. The low proviral load demonstrated in these studies prompts the question of whether LLV failed to grow due to a lack of replication-competent virions. It is also possible that innate restriction factors, such as TRIM5alpha and APOBEC3G, described in other natural lentiviral hosts prevented the virus from infecting domestic cat cells, although the virus also failed to grow in PBMCs of lion origin (35). The high degree of interclade genetic polymorphism among strains suggests that LLV is an ancient lentivirus. Possible host mechanisms that may have evolved to survive viral infection include effective immunologic control, receptor down regulation, and intracellular blocks to replication. It is also possible that the

virus itself has self-selected over time to favor a disease which is relatively apathogenic, allowing hosts to live a normal life span. This situation is similar to that observed for nonpathogenic African SIV, which apparently does not cause disease in native hosts, and may signify the evolutionary outcome of prolonged lentiviral-host adaptation (3, 7, 14). Interestingly, several case studies of naturally occurring SIV disease in African monkeys have been recorded and are consistent with our findings that disease occurs only in animals in captivity that have aged beyond the typical life span of free-ranging animals (24, 27, 33, 49).

This study demonstrates that LLV infection was associated with neuropathy and immune dysregulation, leading to end-stage disease in three captive lions. This finding holds significant health consequences for free-ranging and captive lions, given their endangered status and limited ability to outbreed. It also suggests several new directions for LLV research. It has already been demonstrated that the inoculation of domestic cats with LLV provides protection from subsequent FIV type B infection (54). Determination of the plasma viral load or the level of tissue viremia relative to the proviral load may be informative for the transcriptional control of LLV during infection. Similarly, evaluation of the cell types infected by LLV could direct studies of innate restriction to viral replication and receptor usage. Studies of LLV both in vivo and in vitro could therefore provide information about host control and viral adaptation of lentiviral infection, as well as the correlates of pathogenesis.

ACKNOWLEDGMENTS

We thank the Columbus Zoo keepers and veterinary staff for caring for these animals and to Broad Street Imaging, Columbus, OH, for performing MRI examinations. The tissue samples from lion DJ were evaluated by Department of Veterinary BioSciences, College of Veterinary Medicine, Ohio State University (Paul Stromberg and Steven Weisbrode).

This work was funded by the Cooperative Grants Program, Columbus Zoo, and Ohio State University and by the Merck-Merial Summer Fellowship Program.

REFERENCES

1. **Ackley, C. D., and M. D. Cooper.** 1992. Characterization of a feline T-cell-specific monoclonal antibody reactive with a CD5-like molecule. Am. J. Vet. Res. **53:**466–471.
2. **Bakker, L. J., H. S. Nottet, N. M. de Vos, L. de Graaf, J. A. Van Strijp, M. R. Visser, and J. Verhoef.** 1992. Antibodies and complement enhance binding and uptake of HIV-1 by human monocytes. AIDS **6:**35–41.
3. **Broussard, S. R., S. I. Staprans, R. White, E. M. Whitehead, M. B. Feinberg, and J. S. Allan.** 2001. Simian immunodeficiency virus replicates to high levels in naturally infected African green monkeys without inducing immunologic or neurologic disease. J. Virol. **75:**2262–2275.
4. **Brown, E. W., N. Yuhki, C. Packer, and S. J. O'Brien.** 1994. A lion lentivirus related to feline immunodeficiency virus: epidemiologic and phylogenetic aspects. J. Virol. **68:**5953–5968.
5. **Bull, M. E., D. G. Gebhard, W. A. Tompkins, and S. Kennedy-Stoskopf.** 2002. Polymorphic expression in the CD8alpha chain surface receptor of African lions (Panthera leo). Vet. Immunol. Immunopathol. **84:**181–189.
6. **Bull, M. E., S. Kennedy-Stoskopf, J. F. Levine, M. Loomis, D. G. Gebhard, and W. A. Tompkins.** 2003. Evaluation of T lymphocytes in captive african lions (Panthera leo) infected with feline immunodeficiency virus. Am. J. Vet. Res. **64:**1293–1300.
7. **Chakrabarti, L. A.** 2004. The paradox of simian immunodeficiency virus infection in sooty mangabeys: active viral replication without disease progression. Front. Biosci. **9:**521–539.
8. **Chiang, F. L., I. Walot, R. M. Sinow, and C. M. Mehringer.** 1998. Diagnostic imaging of the brain in acquired immunodeficiency syndrome (AIDS). Semin. Ultrasound CT MR **19:**133–153.
9. **Conant, K., A. Garzino-Demo, A. Nath, J. C. McArthur, W. Halliday, C. Power, R. C. Gallo, and E. O. Major.** 1998. Induction of monocyte chemoattractant protein-1 in HIV-1 Tat-stimulated astrocytes and elevation in AIDS dementia. Proc. Natl. Acad. Sci. USA **95:**3117–3121.
10. **Cosenza, M. A., M. L. Zhao, Q. Si, and S. C. Lee.** 2002. Human brain parenchymal microglia express CD14 and CD45 and are productively infected by HIV-1 in HIV-1 encephalitis. Brain Pathol. **12:**442–455.
11. **Dean, G. A., G. H. Reubel, P. F. Moore, and N. C. Pedersen.** 1996. Proviral burden and infection kinetics of feline immunodeficiency virus in lymphocyte subsets of blood and lymph node. J. Virol. **70:**5165–5169.
12. **Diesing, T. S., S. Swindells, H. Gelbard, and H. E. Gendelman.** 2002. HIV-1-associated dementia: a basic science and clinical perspective. AIDS Read. **12:**358–368.
13. **Dua, N., G. Reubel, P. F. Moore, J. Higgins, and N. C. Pedersen.** 1994. An experimental study of primary feline immunodeficiency virus infection in cats and a historical comparison to acute simian and human immunodeficiency virus diseases. Vet. Immunol. Immunopathol. **43:**337–355.
14. **Dunham, R., P. Pagliardini, S. Gordon, B. Sumpter, J. Engram, A. Moanna, M. Paiardini, J. N. Mandl, B. Lawson, S. Garg, H. McClure, Y. X. Xu, C. Ibegbu, K. Easley, N. Katz, I. Pandrea, C. Apetrei, D. L. Sodora, S. I. Staprans, M. B. Feinberg, and G. Silvestri.** 2006. The AIDS resistance of naturally SIV-infected sooty mangabeys is independent of cellular immunity to the virus. Blood **108:**209–217.
15. **Dyrhol-Riise, A. M., P. Voltersvik, O. G. Berg, J. Olofsson, S. Kleivbo, and B. Asjo.** 2001. Residual human immunodeficiency virus type 1 infection in lymphoid tissue during highly active antiretroviral therapy: quantitation and virus characterization. AIDS Res. Hum. Retrovir. **17:**577–586.
16. **Fine, S. M., R. A. Angel, S. W. Perry, L. G. Epstein, J. D. Rothstein, S. Dewhurst, and H. A. Gelbard.** 1996. Tumor necrosis factor alpha inhibits glutamate uptake by primary human astrocytes. Implications for pathogenesis of HIV-1 dementia. J. Biol. Chem. **271:**15303–15306.
17. **Gardner, M. B., and P. A. Luciw.** 1989. Animal models of AIDS. FASEB J. **3:**2593–2606.
18. **Goldstein, S., R. Engle, R. A. Olmsted, V. M. Hirsch, and P. R. Johnson.** 1990. Detection of SIV antigens by HIV-1 antigen capture immunoassays. J. Acquir. Immune Defic. Syndr. **3:**98–102.
19. **Hofmann-Lehmann, R., D. Fehr, M. Grob, M. Elgizoli, C. Packer, J. S. Martenson, S. J. O'Brien, and H. Lutz.** 1996. Prevalence of antibodies to feline parvovirus, calicivirus, herpesvirus, coronavirus, and immunodeficiency virus and of feline leukemia virus antigen and the interrelationship of these viral infections in free-ranging lions in east Africa. Clin. Diagn. Lab. Immunol. **3:**554–562.
20. **Holznagel, E., S. Norley, S. Holzammer, C. Coulibaly, and R. Kurth.** 2002. Immunological changes in simian immunodeficiency virus (SIV_{agm})-infected African green monkeys (AGM): expanded cytotoxic T lymphocyte, natural killer and B cell subsets in the natural host of SIV_{agm}. J. Gen. Virol. **83:**631–640.
21. **Kennedy, J. M., A. Hoke, Y. Zhu, J. B. Johnston, G. van Marle, C. Silva, D. W. Zochodne, and C. Power.** 2004. Peripheral neuropathy in lentivirus infection: evidence of inflammation and axonal injury. AIDS **18:**1241–1250.
22. **Kennedy-Stoskopf, S., D. H. Gebhard, R. V. English, L. H. Spelman, and M. Briggs.** 1994. Clinical implications of feline immunodeficiency virus infection in African lions (Panthera leo): preliminary findings, p. 345–364. Proceedings of the American Association of Zoo Veterinarians. American Association of Zoo Veterinarians, Yulee, Fla.
23. **Lee, S. J., T. Zhou, C. Choi, Z. Wang, and E. N. Benveniste.** 2000. Differential regulation and function of Fas expression on glial cells. J. Immunol. **164:**1277–1285.
24. **Ling, B., C. Apetrei, I. Pandrea, R. S. Veazey, A. A. Lackner, B. Gormus, and P. A. Marx.** 2004. Classic AIDS in a sooty mangabey after an 18-year natural infection. J. Virol. **78:**8902–8908.
25. **Lutz, H., E. Isenbugel, R. Lehmann, R. H. Sabapara, and C. Wolfensberger.** 1992. Retrovirus infections in non-domestic felids: serological studies and attempts to isolate a lentivirus. Vet. Immunol. Immunopathol. **35:**215–224.
26. **Masliah, E., R. M. DeTeresa, M. E. Mallory, and L. A. Hansen.** 2000. Changes in pathological findings at autopsy in AIDS cases for the last 15 years. AIDS **14:**69–74.
27. **McClure, H. M., D. C. Anderson, T. P. Gordon, A. A. Ansari, P. N. Fultz, S. A. Klumpp, P. Emau, and M. Isahakia.** 1992. Natural simian immunodeficiency virus infection in nonhuman primates. Top. Primatol **3:**425–438.
28. **Morgello, S., L. Estanislao, D. Simpson, A. Geraci, A. DiRocco, P. Gerits, E. Ryan, T. Yakoushina, S. Khan, R. Mahboob, M. Naseer, D. Dorfman, and V. Sharp.** 2004. HIV-associated distal sensory polyneuropathy in the era of highly active antiretroviral therapy: the Manhattan HIV Brain Bank. Arch. Neurol. **61:**546–551.
29. **Murayama, Y., A. Amano, R. Mukai, H. Shibata, S. Matsunaga, H. Takahashi, Y. Yoshikawa, M. Hayami, and A. Noguchi.** 1997. CD4 and CD8 expressions in African green monkey helper T lymphocytes: implication for resistance to SIV infection. Int. Immunol. **9:**843–851.
30. **Neuenburg, J. K., H. R. Brodt, B. G. Herndier, M. Bickel, P. Bacchetti, R. W. Price, R. M. Grant, and W. Schlote.** 2002. HIV-related neuropathology, 1985 to 1999: rising prevalence of HIV encephalopathy in the era of highly active antiretroviral therapy. J. Acquir. Immune Defic. Syndr. **31:**171–177.
31. **Oehmichen, M., I. Theuerkauf, and C. Meissner.** 1999. Is traumatic axonal

injury (AI) associated with an early microglial activation? Application of a double-labeling technique for simultaneous detection of microglia and AI. Acta Neuropathol. (Berlin) **97:**491–494.
32. **Olmsted, R. A., R. Langley, M. E. Roelke, R. M. Goeken, D. Adger-Johnson, J. P. Goff, J. P. Albert, C. Packer, M. K. Laurenson, T. M. Caro, et al.** 1992. Worldwide prevalence of lentivirus infection in wild feline species: epidemiologic and phylogenetic aspects. J. Virol. **66:**6008–6018.
33. **Pandrea, I., R. Onanga, P. Rouquet, O. Bourry, P. Ngari, E. J. Wickings, P. Roques, and C. Apetrei.** 2001. Chronic SIV infection ultimately causes immunodeficiency in African non-human primates. AIDS **15:**2461–2462.
34. **Patton, H. K., Z. H. Zhou, J. K. Bubien, E. N. Benveniste, and D. J. Benos.** 2000. gp120-induced alterations of human astrocyte function: Na^+/H^+ exchange, K^+ conductance, and glutamate flux. Am. J. Physiol. Cell Physiol. **279:**C700–C708.
35. **Perez, O., and T. J. Hope.** 2006. Cellular restriction factors affecting the early stages of HIV replication. Curr. HIV/AIDS Rep. **3:**20–25.
36. **Phipps, A. J., K. A. Hayes, W. R. Buck, M. Podell, and L. E. Mathes.** 2000. Neurophysiologic and immunologic abnormalities associated with feline immunodeficiency virus molecular clone FIV-PPR DNA inoculation. J. Acquir. Immune Defic. Syndr. **23:**8–16.
37. **Podell, M., K. Hayes, M. Oglesbee, and L. Mathes.** 1997. Progressive encephalopathy associated with CD4/CD8 inversion in adult FIV-infected cats. J. Acquir. Immune Defic. Syndr. Hum. Retrovirol. **15:**332–340.
38. **Podell, M., P. A. March, W. R. Buck, and L. E. Mathes.** 2000. The feline model of neuroAIDS: understanding the progression towards AIDS dementia. J. Psychopharmacol. **14:**205–213.
39. **Podell, M., K. Maruyama, M. Smith, K. A. Hayes, W. R. Buck, D. S. Ruehlmann, and L. E. Mathes.** 1999. Frontal lobe neuronal injury correlates to altered function in FIV-infected cats. J. Acquir. Immune Defic. Syndr. **22:** 10–18.
40. **Podell, M., M. Oglesbee, L. Mathes, S. Krakowka, R. Olmstead, and L. Lafrado.** 1993. AIDS-associated encephalopathy with experimental feline immunodeficiency virus infection. J. Acquir. Immune Defic. Syndr. **6:**758–771.
41. **Podell, M., R. Wack, and S. VandeWoude.** 1999. Neurological complications of FIV in lions, p. 256–260. Proceedings of the American Association of Zoo Veterinarians. American Association of Zoo Veterinarians, Yulee, Fla.
42. **Poli, A., F. Abramo, P. Cavicchio, P. Bandecchi, E. Ghelardi, and M. Pistello.** 1995. Lentivirus infection in an African lion: a clinical, pathologic and virologic study. J. Wildl. Dis. **31:**70–74.
43. **Post, M. J., B. E. Levin, J. R. Berger, R. Duncan, R. M. Quencer, and G. Calabro.** 1992. Sequential cranial MR findings of asymptomatic and neurologically symptomatic HIV+ subjects. Am. J. Neuroradiol. **13:**359–370.
44. **Rhodes, R. H.** 1991. Evidence of serum-protein leakage across the blood-brain barrier in the acquired immunodeficiency syndrome. J. Neuropathol. Exp. Neurol. **50:**171–183.
45. **Rodrigo, A. G., P. C. Goracke, K. Rowhanian, and J. I. Mullins.** 1997. Quantitation of target molecules from polymerase chain reaction-based limiting dilution assays. AIDS Res. Hum. Retrovir. **13:**737–742.
46. **Roelke, M. E., J. Pecon-Slattery, S. Taylor, S. Citino, E. Brown, C. Packer, S. VandeWoude, and S. J. O'Brien.** 2006. T-lymphocyte profiles in FIV infected wild lions and pumas reveal CD4 depletion. J. Wildl. Dis. **42:**234–248.
47. **Safriel, Y. I., J. O. Haller, D. R. Lefton, and R. Obedian.** 2000. Imaging of the brain in the HIV-positive child. Pediatr. Radiol. **30:**725–732.
48. **Sleasman, J. W., and M. M. Goodenow.** 2003. HIV-1 infection. J. Allergy Clin. Immunol. **111:**S582–S592.
49. **Souquiere, S., F. Bibollet-Ruche, D. L. Robertson, M. Makuwa, C. Apetrei, R. Onanga, C. Kornfeld, J. C. Plantier, F. Gao, K. Abernethy, L. J. White, W. Karesh, P. Telfer, E. J. Wickings, P. Mauclere, P. A. Marx, F. Barre-Sinoussi, B. H. Hahn, M. C. Muller-Trutwin, and F. Simon.** 2001. Wild *Mandrillus sphinx* are carriers of two types of lentivirus. J. Virol. **75:**7086–7096.
50. **Spencer, J. A., A. A. Van Dijk, M. C. Horzinek, H. F. Egberink, R. G. Bengis, D. F. Keet, S. Morikawa, and D. H. Bishop.** 1992. Incidence of feline immunodeficiency virus reactive antibodies in free-ranging lions of the Kruger National Park and the Etosha National Park in southern Africa detected by recombinant FIV p24 antigen. Onderstepoort J. Vet. Res. **59:**315–322.
51. **Swofford, D. L.** 1998. PAUP*: phylogenetic analysis using parsimony (*and other methods). Sinauer, Sunderland, Mass.
52. **Troyer, J. L., J. Pecon-Slattery, M. E. Roelke, L. Black, C. Packer, and S. J. O'Brien.** 2004. Patterns of feline immunodeficiency virus multiple infection and genome divergence in a free-ranging population of African lions. J. Virol. **78:**3777–3791.
53. **Troyer, J. L., J. Pecon-Slattery, M. E. Roelke, W. Johnson, S. VandeWoude, N. Vazquez-Salat, M. Brown, L. Frank, R. Woodroffe, C. Winterbach, H. Winterbach, G. Hemson, M. Bush, K. A. Alexander, E. Revilla, and S. J. O'Brien.** 2005. Seroprevalence and genomic divergence of circulating strains of feline immunodeficiency virus among *Felidae* and *Hyaenidae* species. J. Virol. **79:**8282–8294.
54. **VandeWoude, S., C. A. Hageman, S. J. O'Brien, and E. A. Hoover.** 2002. Nonpathogenic lion and puma lentiviruses impart resistance to superinfection by virulent feline immunodeficiency virus. J. Acquir. Immune Defic. Syndr. **29:**1–10.
55. **VandeWoude, S., S. J. O'Brien, K. Langelier, W. D. Hardy, J. P. Slattery, E. E. Zuckerman, and E. A. Hoover.** 1997. Growth of lion and puma lentiviruses in domestic cat cells and comparisons with FIV. Virology **233:**185–192.
56. **Watkins, L. R., and S. F. Maier.** 2002. Beyond neurons: evidence that immune and glial cells contribute to pathological pain states. Physiol. Rev. **82:**981–1011.
57. **Wei, Q., A. Javadian, N. Lausen, and P. N. Fultz.** 2000. Distribution and quantification of human immunodeficiency virus type 1, strain JC499, proviral DNA in tissues from an infected chimpanzee. Virology **276:**59–69.
58. **Willey, R. L., D. H. Smith, L. A. Lasky, T. S. Theodore, P. L. Earl, B. Moss, D. J. Capon, and M. A. Martin.** 1988. In vitro mutagenesis identifies a region within the envelope gene of the human immunodeficiency virus that is critical for infectivity. J. Virol. **62:**139–147.
59. **Yeh, M. W., M. Kaul, J. Zheng, H. S. Nottet, M. Thylin, H. E. Gendelman, and S. A. Lipton.** 2000. Cytokine-stimulated, but not HIV-infected, human monocyte-derived macrophages produce neurotoxic levels of L-cysteine. J. Immunol. **164:**4265–4270.